Journal of Applied Sciences Research, 6(12): 2280-2289, 2010

The Corrosion Behavior of Electroless Ni-P-SiC and Ni-Sn-P-SiC Nano-Composite Coating.

O.R.M. Khalifa; E. Abd El-Wahab and Amal. H. Tilp

Chemistry department, Faculty of Girls for Arts, Science and Education, Ain shams University, Cairo, Egypt.

Abstract: Electroless nickel (EN) and EN composite with SiC and Sn-SiC were deposited by chemical deposition. The microstructure analysis was conducted with scanning electron microscopy, Thin film indicated that the presence of SiC particles did not affect the microstructure of the Ni- P alloy matrix when annealing temperature was below 400°C. EDAX (Energy dispersive x-ray analysis) technique have been applied in order to investigate the chemical composition and indicated that linear relation between SiC concentrations and SiC content. Microhardness of electroless Ni-Sn-P deposite, Ni-P-SiC composite and Ni-Sn-P-SiC composite were studied. Microhardness reached to the maximum value after heating to 400ºC for 1h. Microhardness follow the sequence Ni-P-SiC > Ni-Sn-P-SiC > Ni-P > Ni-Sn-P. Finally, the corrosion resistance of different SiC content and constant concentration of SnCl2 was studied in different corrosive solutions (1M H2SO4 and 3.5% NaCl solution).

Kew words: Electroless, Nano-composite, coating

INTRODUCTION

Since the invention of electroless plating technology in 1946 by A.Brenner and G.Riddell electroless nickel coatings have been used in many fields due to its unique properties. The structure of electroless Ni-P as deposited is amorphous with high phosphorus content. However, this amorphous structure is metastable and under goes a crystalline transition with temperature increase[1-6] after adequate heat treatment, the coating turned to crystal and its hardness improved greatly. Electroless composite plating is a kind of surface treatment technology developed on the basis of electroless plating prepared by adding solid particles to the regular electroless Ni-P plating solution [eg. Al_2O_3[7], B_4C[8], WC[9], SiC[10], diamond[11] or soft MoS_2[12], PTFE[13] and graphite particles to achieve co deposition of the solid particles and Ni-P matrix and improves the mechanical and tri biological properties of Ni-P coating[14-18]. Such coatings with high corrosion resistance, wear resistance and uniform coating thickness have found wide applications in the industries of aviation, aerospace, electronics, petroleum, chemistry machinery, textiles and automotives[19-20].

This work aimed to obtain amorphous Ni-P coating containing crystalline SiC nm particles. The effect of SiC particles and 0.05g/l of $SnCl_2$ solution on the coating properties was discussed.

Experimental methods

2.1. Test material:

Specimen prepared from low carbon steel

Element	C	Mn	Si	P	S	other	Fe
wt%	0.26	0.6	0.08	0.008	0.006	<0.01	Rest

2.2. Test procedures: Pretreating of specimen → removing oil with absolute ethyl alchol (for 5-20minutes) → removing oil with alkali (at 80-90°C for 2 minutes)→ flushing with hot water → scrupling with water → preheating → elctroless composite plating → flushing with hot water → flushing with cold water → drying → weighing.

2.3. The composition of electroless plating solution and the process conditions are listed in table (1): The composite coating were deposited from the most stable baths containing SiC powder with concentrations of 4,6,8 and 10 g/l. Available SiC particles with a mean size of 129.4 nm were used. The bath composition and operation conditions used for preparing Ni-P-SiC and Ni-Sn-P-SiC composite coatings are given in table (1). The bath was stirred by a rotating stirring rod with a rate of 3 rpm. The deposition process was carried out for 1 h, at constant temperature 80-83°C.

Corresponding Author: Dr. (Mrs) S.M.O. Akhionbare, Department of Project Management Tech., E-mail: smoakhionbare2007@yahoo.com

RESULTS AND DISCUSSION

3.1. Thin film (PANlytical, X pert PRO): The layer of Ni-P, Ni-Sn-P, Ni-P-SiC and Ni-Sn-SiC-P coatings are shown in Fig (1). It is found that the structure of these type of coatings exhibiting a nickel matrix in the range of 2θ corresponding to the amorphous matrix of Ni-P layer. For Ni-P-SiC and Ni-Sn-P-SiC composites, there are some small sharp peaks. Those sharp small peaks corresponds to the position of crystalline SiC .It is confirmed that structural changes from amorphous state to crystalline state can be obtained in Ni-P electroless coatings over 250ºC[21]. Fig (2) shows that the phase of different alloys coatings after heat treatment at 400°C for 1 hour leads to complete crystallization of amorphous matrix the superfine particles do not change the structure of Ni-P alloy during electroless plating .As shown in fig (2) the electroless composite coating crystallized into nickel crystal (Ni), nickel phosphide (Ni_3P), nickel silicates (Ni_xSi_y), and tin phosphide (SnP) and SiC.

3.2. Scanning electron microscope (surface morphology) (JEOL JSM 5410, Japan): Fig (3) showes the SEM picture of EN and EN composite coatings. EN Sn, EN SiC and EN Sn SiC were deposited with tin chloride solution and SiC particles suspended in the bath. The surface morphology of EN and EN Sn deposit showed spherical nodular cluster shape with nano structure [22] and [23] Fig (3) a and b. Superfine SiC particles were successfully co-deposited in Ni-P alloy matrix by electroless plating with the increase of SiC in the bath, the content of particles in the coating increase but the plating rate decreased. Observed by the nacked eye, the composite coatings are smooth and bright as deposit.

It can be seen that superfine SiC particles were successfully co-deposited in Ni-P alloy matrix by electroless plating. The morphology of Ni-P-SiC shows a relatively big and (boomerang-type) irregular shaped SiC particles are evently distributed within the coating and are enveloped.The embedded SiC grains into the amorphous matrix distincitly enlarge the surface development of the composite Ni-P-SiC layer compared with Ni-P and Ni-Sn-P.

Fig (4) shows the morphology of EN, EN- Sn, EN- SiC and EN- Sn- SiC after heat treatment to 400°C for one hour, the Si—C bonds are broken and Ni atoms displace the C atom, then nickel silicates (simply expressed as Ni_xSi_y).

Fig (4) a and b show Ni-P and Ni-Sn-P alloy after heat treatment with cluster nano structure. Fig (4) c and d show Ni-P-SiC and Ni-Sn-P-SiC the embedded SiC grains distinctly enlarge the surface of the composite Ni-Sn-P-SiC compared with Ni-P.

3.3. EDAX analysis: EDAX analysis technique was used to determine the chemical composition of the produced coatings.

Fig (5) shows the relationship between the weight percentage (wt %) of the codeposited SiC particles into the composite coatings and the content of the powder in the plating bath at stirring rate of 3 rpm. From Fig (5) SiC content in coating increases with increasing of SiC content in the bath .For SiC concentration lower than 9 g/l, there is a sharp increase of SiC content in coating with the increase of SiC in the bath this is because of the effective concentration of SiC particles in the bath increases and the deposition of SiC particles on the coating surface accelerates accordingly due to the agitating action, at content of SiC higher than 8 g/l in the bath, a slight increase of SiC content in the coating deposite, because the congregation among particles in solution tend to be striking when the particle content increases to a certain degree The floatability of congregating SiC particles is weakened because of weight increasing (saturation value). Hence, the increment of effective SiC concentration decreases and SiC content in the coating will increase slowly. At high concentration of SiC particles, the distribution density of the SiC particles on the substrate surface increases which leads to the isolation of the surface and decrease the deposition rate.

Electrochemical study:

3.4.1. Corrosion resistance: To find out the electrochemical behaviour of coatings Ni-P, Ni-Sn-P, Ni-P-SiC and Ni-Sn-P-SiC, potentiodynamic polarization studies were carried out in artificial sea water 3.5% NaCl and 1 M H_2SO_4 solutions.

Potentiodynamic curves of composite of four different SiC content (4, 6, 8 and 10 g/l) in artificial sea water (3.5% NaCl) and in 1M H_2SO_4 solutions are shown in Figs (6) and (7). The electrochemical corrosion parameters obtained from the Tafel polarization curves are listed in tables (5-8). From Figs (6) and (7).all the coatings have showed relatively good resistance to corrosion in sodium chloride and H_2SO_4 solutions.

Potentiodynamic polarization curves of composite coatings of four different SiC contents (4,6,8 and 10 g/l) in 3.5% NaCl solution are shown in fig (6), with the increase of SiC content in coating the corrosion resistance of electroless Ni-P-SiC composite coatings decreases gradually. The Electroless Ni-P coating is a kind of amorphous structure alloy with high corrosion resistance. When SiC add, insoluble solid particles, are embedded in electroless Ni-P coating, crystal boundary and dislocation well appear at the interface between SiC particle and Ni-P alloy due to the difference of particle size and surface conditions of them. This

produces different electric potentials at different places of coating soaked in corrosive medium and thus micro cell forms. The micro cell causes intergranular corrosion, namely electrochemical corrosion. Therefore the corrosion resistance of electroless Ni-P-SiC composite coating decreases with the increase of SiC content [24] and [25].

The high corrosion protection of Ni-P and Ni-Sn-P could be due to the nano grain size of the binary alloy (grain size is 3.6nm) and the ternary alloy Ni-Sn-P (grain size is 5.1nm) in good agreement with previous author [23]. This means that the binary Ni-P and ternary Ni-Sn-P form a surface protective film with absence of defects in crystalline alloys

Table 1: Composition of electroless plating solution and plating conditions.

Plating bath composition	Ni-P	Ni-P-SiC	Ni-Sn-P	Ni-Sn-P-SiC
$NiSO_4$.$7H_2O$	30 g/l	30 g/l	30 g/l	30 g/l
$NaH_2PO_2.H_2O$	25 g/l	25 g/l	25 g/l	25 g/l
$CH_3COONa._3H2O$	20 g/l	20 g/l	20 g/l	20 g/l
Lactic acid	10 ml /l	10 ml /l	10 ml /l	10 ml /l
Propionic acid	10 ml /l	10 ml /l	10 ml /l	10 ml /l
Surfactant (g/l)	0.2 g /l	0.2 g /l	0.2 g /l	0.2 g /l
$SnCl_2$ (g/l)	-	-	0.05 g/l	0.05 g/l
SiC powder (g/l)	-	4-10 g/l	-	4-10 g/l
pH	5	5	5	5
Plating temperature (ºC)	80-83	80-83	80-83	80-83
Agitation method		Magnetic strrier (3rpm)		Magnetic strrier (3rpm)
Coating time	1h	1h	1h	1h

Table 2: Peak position (2θ), full width at half maximum and grain size (from Debye-Scherrer formula) for as plated electroless Ni-P, Ni-Sn-P, Ni-P-SiC and Ni-Sn-P-SiC coatings

Type of coating	Before heat treatment		After heat treatment at 400ºC	
	Peak position	Grain Size(nm)	Peak position	Grain Size(nm)
Ni-P	44.50	3.6	44.51	41.4
Ni-Sn-P	45.56	5.1	44.51	59.2
Ni-P-SiC	35.63	7.8	44.48	73.2
Ni-Sn-P-SiC	35.63	11.1	44.44	96.2

Table 3: The atomic percentage of the constituent element in Ni-P-SiC different contents (4, 6, 8 and 10 g/l).

contents of SiC g/l	wt percent (wt%)		
	P	SiC	Ni
4	12.5	5.8	81.7
6	12	10	78
8	10	14.5	75.5
10	9	16.5	74.5

Table 4: Composition of as-plated electroless nickel alloy coating determined by EDAX analysis.

Type of coatings	Weight percent			
	Ni	SiC	Sn	P
Ni-P	89.38	-	-	10.62
Ni-Sn-P	90.20	-	0.6	9.2
Ni-P-SiC	74.5	16.5	-	9
Ni-Sn-P-SiC	91.0	0.6	0.9	7.5

Table 5: The corrosion kinetic parameters E_{corr}, I_{corr}, Corrosion rate(MPY) and R_p, determined from the in the Tafel region, for different SiC concentrations (4, 6, 8 and 10 g/l) in 3.5% sodium chloride solution.

Concentrations	E_{corr}	I_{corr}	C.R. (MPY)	R_P	β_a	β_c
Ni-P	-0.389	2.549×102	0.237×103	6.295×104	0.187	0.046
4g/l SiC	-0.406	4.651×103	4.328×103	6.214×103	0.238	0.093
6g/l SiC	-0.435	5.151×103	4.793×103	6.141×103	0.123	0.178
8g/l SiC	-0.464	6.045×103	5.625×103	3.966×103	0.102	0.123
10g/l SiC	-0.478	8.108×103	7.545×103	2.633×103	0.144	0.08

Table 6: The corrosion kinetic parameters E_{corr}, I_{corr}, Corrosion rate (MPY) and R_p, determined from the polarization curves in the Tafel region, for different SiC concentrations (4, 6, 8 and10 g/l) in 1M sulphuric acid solution.

Concentrations	Ecorr	Icorr	C.R. (MPY)	R_p	β_a	β_c
Ni-P	-0.381	4.375×105	4.071×105	0.0618×103	0.144	0.11
4g/l SiC	-0.382	5×105	4.653×105	0.0543×103	0.17	0.102
6g/l SiC	-0.397	1.093×106	10.172×105	0.0291×103	0.106	0.263
8g/l SiC	-0.485	4.509×106	41.963×105	0.0116×103	0.208	0.297
10g/l SiC	-0.493	5.781×106	53.801×105	0.0015×103	0.021	0.421

Table 7: The corrosion kinetic parameters E_{corr}, I_{corr}, Corrosion rate(MPY) and R_p, determined from the polarization curves in the Tafel region, for different Ni-P-0.05g/l$SnCl_2$-SiC (4, 6,8 and10 g/l) content in 3.5%sodium chloride solution.

Concentrations	E_{corr}	I_{corr}	C.R. (MPY)	R_p	β_a	β_c
4g/l SiC+ 0.05g/l SnCl2	-0.261	1.960×102	0.182×103	1.010×105	0.153	0.068
6g/l SiC+ 0.05g/l SnCl2	-0.265	3.461×102	0.322×103	5.696×104	0.072	0.127
8g/l SiC+ 0.05g/l SnCl2	-0.296	4.313×102	0.401×103	2.836×104	0.251	0.034
10g/l SiC+ 0.05g/l SnCl2	-0.402	8.139×102	7.574×103	4.683×103	0.157	0.208

Table 8: The corrosion kinetic parameters E_{corr}, I_{corr}, Corrosion rate(MPY) and R_p, determined from the polarization curves in the Tafel region, for different Ni-P-0.05g/l$SnCl_2$-SiC (4,6,8 and10 g/l) content in 1 M sulphuric acid solution.

Concentrations	E_{corr}	I_{corr}	C.R. (MPY)	R_p	β_a	β_c
4g/l SiC+ 0.05g/l SnCl2	-0.313	3.055×105	2.843×105	0.0945×103	0.144	0.127
6g/l SiC+ 0.05g/l SnCl2	-0.328	0.937×106	8.720×105	0.0345×103	0.195	0.127
8g/l SiC+ 0.05g/l SnCl2	-0.387	2.656×106	24.718×105	0.0114×103	0.204	0.11
10g/l SiC+ 0.05g/l SnCl2	-0.417	4.687×106	43.62×105	0.0058×103	0.127	0.127

Table 9: Corrosion characteristic of as plated electroless Ni-P, Ni-Sn-P, Ni-P-SiC and Ni-Sn-P-SiC coatings in 3.5% sodium chloride solution.

Concentrations	E_{corr}	I_{corr}	C.R. (MPY)	R_p
Ni-P	-0.389	2.549×102	0.237×103	6.295×104
Ni-Sn-P	-0.367	1.96×102	0.182×103	6.459×104
Ni-P-SiC	-0.406	4.651×103	4.328×103	6.214×103
Ni-Sn-P-SiC	-0.261	1.960×102	0.182×103	1.010×105

Table 10: Corrosion characteristic of as plated electroless Ni-P, Ni-Sn-P, Ni-P-SiC and Ni-Sn-P-SiC coatings in 1 M sulphuric acid solution.

Concentrations	E_{corr}	I_{corr}	C.R. (MPY)	R_P
Ni-P	-0.381	4.375×105	4.071×105	0.0618×103
Ni-Sn-P	-0.092	0.0125×105	1.163×103	1.4165×104
Ni-P-SiC	-0.382	5×105	4.653×105	0.0543×103
Ni-Sn-P-SiC	-0.313	3.055×105	2.843×105	0.0945×103

3.5. Hardness measurements.

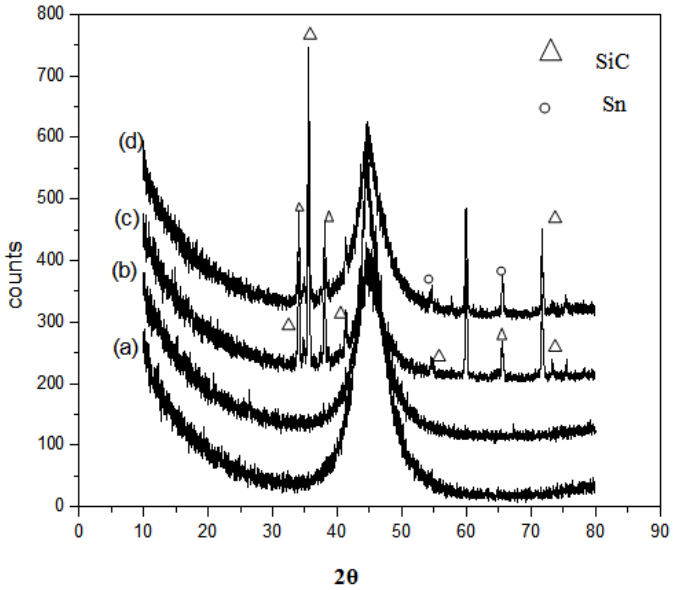

Fig. 1: X-ray diffraction pattern of as plated of electroless (a) Ni-P, (b) Ni-Sn-P, (c) Ni-P-SiC, (d) Ni-Sn-P-SiC before heat treatment.

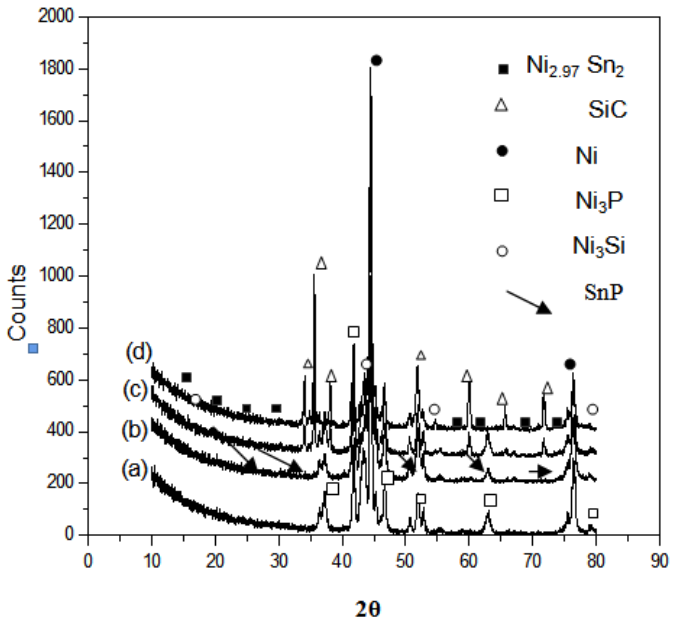

Fig. 2: X-ray diffraction pattern of electroless (a) Ni-P, (b) Ni-Sn-P, (c) Ni-P-SiC, (d) Ni-Sn-P-SiC after heat reatment at 400°C.

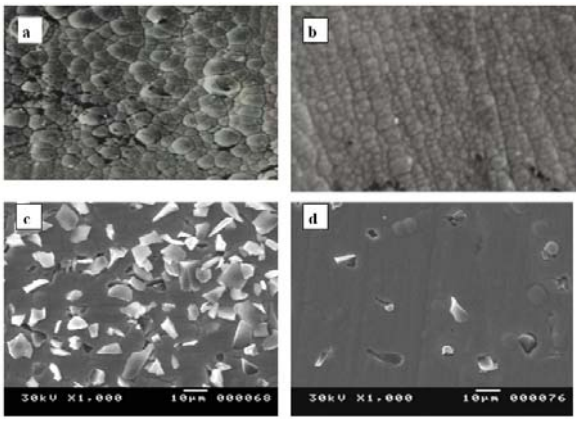

Fig. 3: Scanning electron microscope of as plated electroless (a)Ni-P (b)Ni-Sn-P (c) Ni-P-SiC (d) Ni-Sn-P-SiC before heat treatment.

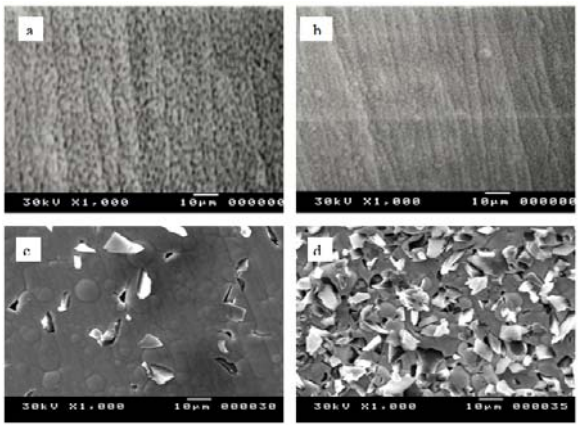

Fig. 4: Scanning electrom microscope of as plated electroless (a)Ni-P (b)Ni-Sn-P (c) Ni-P-SiC (d)Ni-Sn-P-SiC after heat treatment at 400ºC .

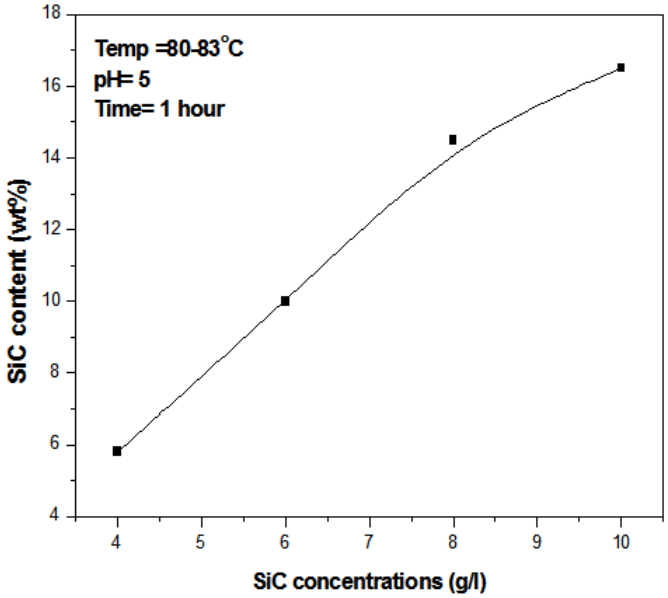

Fig. 5: The relationship between SiC concentration in the bath and SiC content in the coating

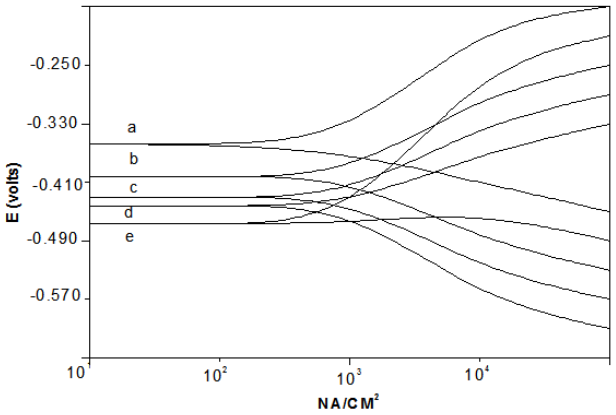

Fig. 6: Potentiodynamic polarization curves of electroless Ni-P coatings as a function of different SiC concentrations (a) Ni-P, (b) 4g/l, (c) 6g/l, (d) 8g/l. (e) 10g/l in 3.5% sodium chloride solution.

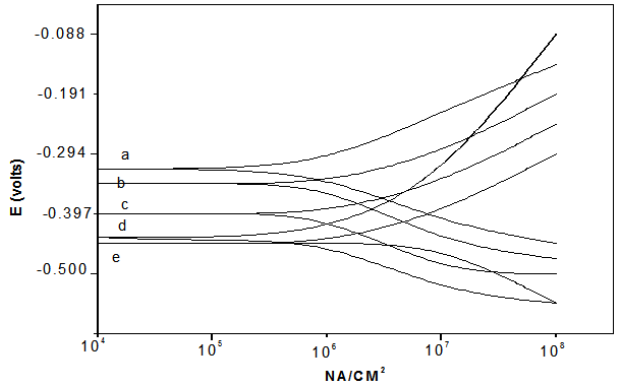

Fig. 7: Potentiodynamic polarization curves of electroless Ni-P coatings as a function of different SiC concentrations (a) Ni-P, (b) 4g/l, (c) 6g/l, (d) 8g/l. (e) 10g/l in 1M sulphuric acid solution.

The quaternary alloy Ni-Sn-SiC-P composite was prepared by using four different SiC content in the plating bath and a constant concentration of tin chloride 0.05 g/l. The results are shown in Figs (8) and (9). At constant content of SiC in the bath free and contain 0.05g/l tin chloride, Potentiodynamic polarization curves show that the presence of tin chloride noticeable shift of the corrosion potential to noble direction in case sodium chloride solution (4g/l SiC, Ni-SiC-P [E_{corr} -0.406volt], Ni-Sn-SiC-P [E_{corr} -0.261volt]) and in case sulphuric acid solution (4g/l SiC, Ni-P-SiC [E_{corr} -0.382 volt], Ni-Sn-P-SiC [E_{corr} -0.313 volt]). This means that presence of tin chloride causes a strong corrosion protection i.e. quaternary alloy Ni-Sn-P-SiC had greater corrosion protection than ternary alloy Ni-P-SiC. AT constant value of SiC (4g/l).Potentiodynamic polarization curves of the quaternary alloy Ni-Sn-P-SiC are shown in figs (10) and (11). The best corrosion protection of the quaternary alloy is Ni-Sn-P-SiC (SiC 4g/l).

As SiC content increase in the quaternary alloy, the corrosion potential increases to more negative values (from -0.261 to -0.401v) the reason is described before.

Hardness measurements: Table (11) gives the microhardness measurements results of as plated and heat treated electroless of nickel alloy deposits. Upon heat treatment, enhancement in hardness for the binary Ni-P coatings can be due to the precipitation of nickel phosphide. From the table, it is evident that the presence of tin in Ni-Sn-P deposit has reduced the hardness value. An increase in hardness values can be seen in ternary Ni-P-SiC and quaternary Ni-Sn-P-SiC coatings. In the case of the ternary Ni-Sn-P coatings, maximum hardness value was attained at HV_{300} 510. This can be attributed to the precipitation of metastable and also solid solution form of tin. Micro hardness values of electroless Ni-P-SiC composite coatings as deposited increase because of the introduction of hard particles and dispersion strength. It is shown that in table (11) that the micro hardness of electroless Ni-P-SiC composite coating raises to the maximum value (about HV_{300}620) after heat treatment at 400ºC for 1 h (about HV_{300} 660).

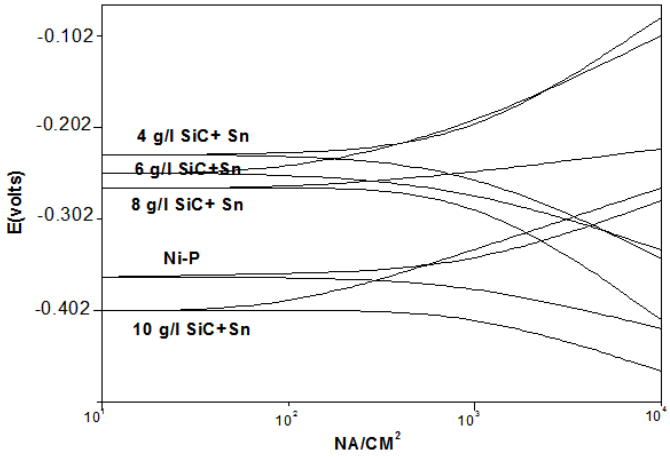

Fig. 8: Potentiodynamic polarization curves of electroless Ni-P coatings as a function of different SiC content+0.05 g/l SnCl2 in 3.5% sodium chloride solution.

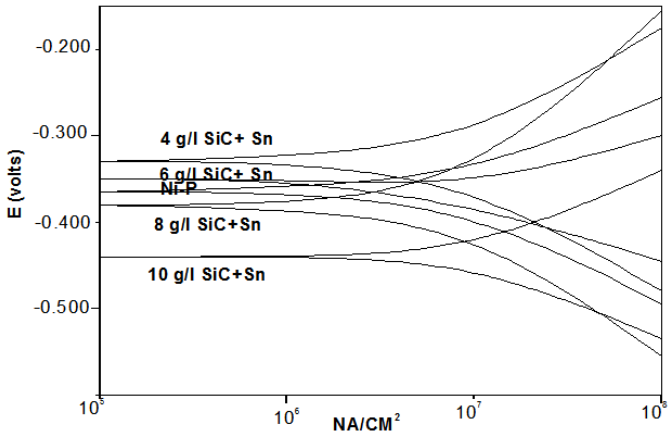

Fig. 9: Potentiodynamic polarization curves of electroless Ni-P coatings as a function of different SiC content +0.05 g/l SnCl2 in 1 M sulphuric acid solution.

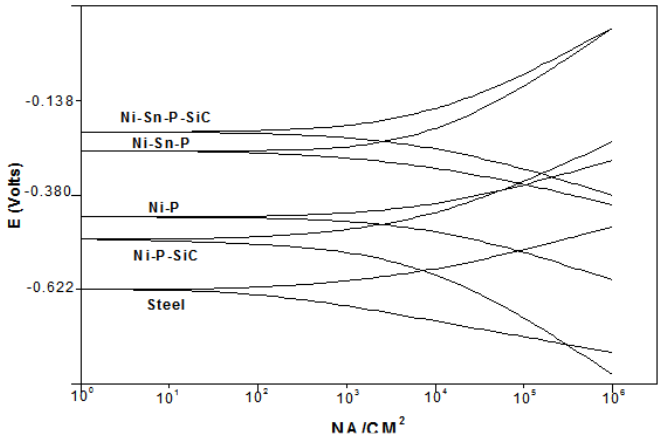

Fig. 10: potentiodynamic polarization curves of as plated Electroless (a) Ni-P, (b) Ni-Sn-P, (c) Ni-P-SiC, (d) i-Sn-P-SiC coatings in 3.5% sodium chloride solution.

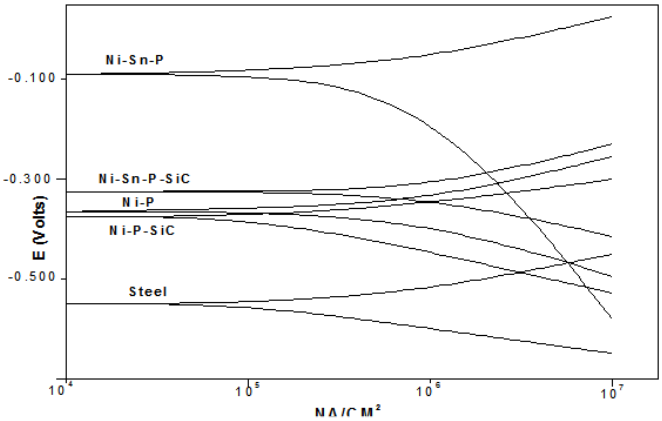

Fig. 11: potentiodynamic polarization curves of as plated Electroless (a) Ni-P, (b) Ni-Sn-P, (c) Ni-P-SiC, (d) i-Sn-P-SiC coatings in 1 M sulphuric acid solution.

Table 11: microhardness of electroless Ni-P alloys as plated and heat treated for 1h at400ºC

Type of coatings	Micro hardness (HV_{300})	
	As plated	Heat treatment at 400ºC
Ni-P	510	450
Ni-Sn-P	400	510
Ni-P-SiC	620	660
Ni-Sn-P-SiC	590	620

For the as deposited quaternary Ni-Sn-P-SiC is greater than as deposited Ni-P and as deposited Ni-Sn-P and less than Ni-P-SiC composite. Upon heating the quaternary Ni-Sn-P-SiC composite has greater hardness than Ni-Sn-P due to form ($Ni_{2.97}$ Sn_2, Ni, SiC, Ni_3Si, and Ni_3P) phases which are more crystalline than (SnP, Ni_3P, Ni, and Sn). Also heated Ni-Sn-P-SiC has less hardness than Ni-P-SiC (Ni, SiC, Ni_3Si, Ni_3P) which are more crystalline than Ni-Sn-P-SiC

Conclusion: Electroless Ni-P-SiC and Ni-Sn-P-SiC composite coatings with superfine SiC particles were prepared by electroless plating. Superfine SiC particles dispersed homogenously and the content of particles was at high level in composite coatings. The structure of the composite coatings as deposited was amorphous. After heating at 400°C, the amorphous alloy in electrless Ni-P-SiC and Ni-Sn-P-SiC composite coatings crystallized, and then reacted with SiC. The final products of the crystallization and reaction of composite coatings were Ni, Ni_3P, Ni_3Si, $Ni_{31}Si_{12}$ and $Ni_{2.97}Sn_2$.

potentiodynamic polarization curves show that the corrosion protection follow the sequence Ni-Sn-P-SiC > Ni-Sn-P > Ni-P > Ni-P-SiC in 3.5% sodium chloride solution while in case sulphuric acid solution Ni-Sn-P > Ni-Sn-P-SiC > Ni-P > Ni-P-SiC. The Microhardness follow the sequence Ni-P-SiC > Ni-Sn-P-SiC > Ni-P > Ni-Sn-P.

REFERENCES

1. Hentschel, T.H. *et al.,* 2000. Acta Mater., 48: 933.
2. Farber, B. *et al.,* 2000. Acta Mater., 48:789.
3. Agarwala, R.C., Z.S. Ray, 1996. Metallkade., 83: 65.
4. Duncan, R.N., 1996. Plat. Surf. Finish., 83: 65.
5. Kwang-Lung Lin, J. Po-Jen Lai, 1989. Electrochem. Soc., 136: 3803.
6. Keong, K.G., W. Sha, S. Malinov, J. Alloy, 2002. Compd., 334: 192.
7. Balarju, J.N., K.S. Kalavati, 2006. Rajam, Surf.Coat. Technol., 200: 3933.
8. Ebrahim. M., K. Hosseinabadi, Azari- S.M. Dorcheh, 2006. Moonir-Vaghefi, wear., 260: 123.
9. Abdel, Z. S.A.Hamid, A. El Badry, 2007. Abdel Aal, Surf.Coat. Technol., 201: 5948.
10. Chen, C.K., H.M. Feng, H.C. Lin, M.H. Hon, 2002. Thin Solid Films., 416: 31.
11. Sheela, G., M., Pushpavanam, 2002. Met. Finish. 1: 45.

12. Moonir- Vaghefi, S.M., A. Saatch, J. Hejazi, 1997. Met. Finish., 95(6): 102.
13. Zhao, Q., Y. Lui, H. Muller-Stanhagen, G. Liu, 2002. Surf. Coat. Tenchnol., 155: 279.
14. Grosjean, A., M. Rezrazi, J. Takadoum, P. Bercot, 2001. Surf. Coat. Technol., 137: 92.
15. Apachitei, I., 2002. Surf. Coat. Technol., 149: 263.
16. Balaraju, J.N., S.K. Seshadri, 1999. Trans. IMF., 77: 84.
17. Ming-Der Ger, 2001. Bing Joe Hwang. Mater. Chem. Phys., 76: 38.
18. Moonir-Vaghefi, S.M., A. Saatchi, J. Hejazi, Z. Met, 1997. Kd., 88: 498.
19. Jin, J.G., S.K. Lee, Y.H. Kim, 2004. Thin Solid Films, 466: 272.
20. Niwa, D., N. Takano, T. Yamada, 2003. Electrochim. Acta., 48: 1295.
21. Dervos, C.T., P. Vassiliou, J. Novakovic, 2004. vaccum heated electroless nickel plated [I] IEE.Trans compon packag Tecnology, 27(1): 131-137.
22. Slijkeman, W.F.J. *et al.,* 1989. J. Appl. P hys. 66: 666.
23. Khalifa, O.R.M., E. Abd El-Wahab, H.A. Mohamed, 2007. TIMS Bulletin, 90.
24. Chi, Y., G.C. Zhan, H.Y. Fan, J.B. Gao, 2001. Applied Science and Tecnology, 28: 45.
25. Mimani, T., S.M. Mayanna, 1996. Surf. Coat. Technol., 79: 246.